

uneventful experiments led to the successful photolysis at liquid-helium temperatures described presently.

An NbNO crystal is oriented with  $H\parallel c$  at 80 K and cooled with liquid helium pumped to 1.7 K. The crystal alignment is checked and the spectrum is recorded before photolysis. The crystal is irradiated until the HbNO EPR spectrum drops to less than 6% of its original intensity within  $\sim 2$  min. No HbNO recombination nor any other spectrum is observed at 1.7 K after irradiation. The residual few percent of HbNO have a number ratio of a:b subunits that is as little as  $2/3$  in an originally fully nitrosylated crystal. A unimolecular HbNO recombination with a rate constant above  $\sim 10^{-4} \text{ s}^{-1}$  would be detected in the experiment after irradiation. The subunit photodissociation quantum yields per photon of light absorbed in the Q band are estimated greater than  $10^{-3}$ . They appear to differ very slightly in the  $\alpha$  and  $\beta$  subunits.

After the liquid helium vaporizes, the spectrum is scanned repetitively as the sample warms up to 85 K. There is little if any ( $\leq 5\%$ ) recombination below 70 K in about 20–30 min. Above 70 K the rate becomes observable and recombination is at least 80% complete by 85 K within 10–20 min at most. The temperature stabilizes at 85 K, and the spectrum changes no further. The  $\alpha:\beta$  number ratio returns to within 1% of its value before photolysis, and the spectra are almost indistinguishable.

The experiment demonstrates rapid HbNO photolysis at 1.7 K where recombination rates are comparatively small. The recombination becomes appreciable above  $\sim 70$  K and increases rapidly with temperature to swamp, apparently, the uncompetitive photolysis at 95 K. The minimum activation energy estimated from the experiment is about  $7 \text{ kJ mol}^{-1}$  ( $600 \text{ cm}^{-1}$ ). Energy barriers of  $10 \text{ kJ mol}^{-1}$  and  $4 \text{ kJ mol}^{-1}$  were found for recombination of carbonmonoxymyoglobin<sup>21,22</sup> and  $-\beta$ -Hb chains,<sup>19</sup> respectively. However, in our HbNO recombination there is apparently no fast low-temperature tunnelling.<sup>19</sup> Measurements of the quantum-yield wavelength dependence and recombination rate determinations at fixed temperatures should be made to understand better the photolysis and recombination mechanisms.

### Conclusions

The EPR spectrum of HbNO made from HbO<sub>2</sub> crystals conforms to the HbO<sub>2</sub> crystal symmetry. The principal  $g$  values and

axes of the  $\alpha$  and  $\beta$  subunits were measured. The spectrum with the field along the tetragonal crystal axis was simulated by a sum of two subunit spectra. One subunit displays both <sup>14</sup>N and [<sup>14</sup>N]histidine hyperfine splittings while the other displays only the <sup>14</sup>N pattern. Association of the  $z$  principal  $g$  axis with the heme normal is consistent with the hemoglobin crystal structures and makes possible a tentative assignment to the  $\alpha$  and  $\beta$  subunits.

The uptake of NO from solution by the  $\alpha$  and  $\beta$  subunits in HbO<sub>2</sub> is crystallographically well-behaved according to EPR studies. It is accompanied by no detectable EPR changes in subunits already bound to NO, and the small differences in the  $\alpha$  and  $\beta$   $g$  values suggest no pH- or phosphate-induced effects. The  $a$  subunits exchange at least twice as fast as  $b$  subunits in the first 1.5 h of treatment yielding about two  $a$  subunits for every one  $b$  subunit. The last  $b$  subunit appears to exchange very slowly, and full nitrosylation is reached after about 48 h.

The temperature and power dependence of the HbNO EPR spectrum has the earmarks of magnetic dipolar interaction between the subunit spins. Transfer of saturation between unlike subunits appears directly in the spectrum. At 4.2 K,  $T_1$  and  $T_2$  are comparable, so that transverse relaxation may also be via heme-heme dipolar interactions. Some of the line-width anisotropy observed must arise from unresolved hyperfine interaction.

Rapid photolysis of HbNO occurs with a quantum yield greater than  $10^{-3}$  at 1.7 K, a temperature at which recombination is not occurring with a unimolecular rate over  $10^{-4} \text{ s}^{-1}$ . As the temperature is raised, no appreciable recombination occurs below 70 K, but it becomes competitive with photolysis above 85 K. A minimum activation energy of  $7 \text{ kJ mol}^{-1}$  is estimated for recombination.

**Acknowledgment** is made to the donors of the Petroleum Research Fund, administered by the American Chemical Society, to the SUNY Research Foundation Joint Awards Council and University Awards Committee. The project is supported in part by NIH Grant No. S07RR07149-05 and -06 awarded by the BRSG Program, Division of Research Resources. We are grateful for the scientific help and advice of Professor Anna Tan-Wilson and for the cooperation of our cryogenics engineer, Mr. Weldon Willard, and the Broome County Red Cross Blood Bank.

## Simple Molecular Orbital Explanation for "Bay-Region" Carcinogenic Reactivity

John P. Lowe\* and B. D. Silverman†

Contribution from the Department of Chemistry, The Pennsylvania State University, University Park, Pennsylvania 16802, and the IBM Thomas J. Watson Research Center, Yorktown Heights, New York 10598. Received October 27, 1980

**Abstract:** Polycyclic aromatic hydrocarbons containing a "bay region" form triol carbonium ions with special ease. This is shown to be due to the fact that such ions can have the  $-\text{CH}^+$  group of the triol ring attached to a carbon atom which is a nearest neighbor to a ring fusion site.

### Introduction

Identification<sup>1-3</sup> of the enhanced carcinogenicity of the 7,8-diol 9,10-epoxide of benzo[*a*]pyrene has focused attention on vicinal diol epoxides as likely candidates for the ultimate carcinogens of polycyclic aromatic hydrocarbons (PAH). Investigation of the relative carcinogenic activity of different PAH has led to the

recognition that diol epoxides on angular benzo rings in which the epoxide ring forms part of a "bay region" are the most reactive of all possible isomeric diol epoxides of a given PAH.<sup>4</sup> The

(1) Borgen, A.; Darvey, H.; Castagnoli, N.; Crocker, T. T.; Rasmussen, R. E.; Yang, I. Y. *J. Med. Chem.* **1973**, *16*, 502-506.

(2) Sims, P.; Grover, P. L.; Swaisland, A.; Pal, K.; Hewer, A. *Nature (London)* **1974**, *252*, 326-328.

(3) Jerina, D. M.; Lehr, R.; Schaeffer-Ridder, M.; Yagi, H.; Karle, J. M.; Thakker, D. R.; Wood, A. W.; Lu, A. Y. H.; Ryan, D.; West, S.; Levin, W.; Conney, A. H. *Cold Spring Harbor Conf. Cell Proliferation* **1977**, *4*, 639-658.

\* Address correspondence to this author at The Pennsylvania State University.

† IBM Thomas J. Watson Research Center.

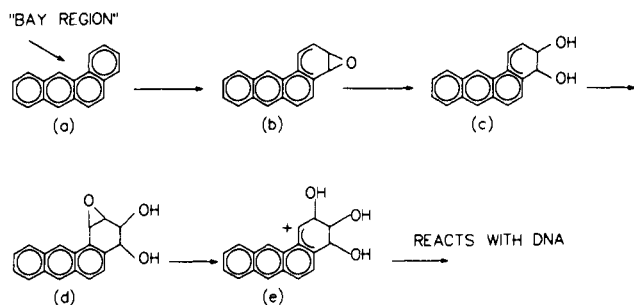


**Figure 1.** Possible reaction sequence producing an ultimate carcinogen wherein benzo[*a*]anthracene (a) forms, in succession, an epoxide (b), a dihydrodiol (c), a dihydrodiol epoxide (d), and a triol carbonium ion (e) which reacts with an amino acid on DNA. (See ref 3.)

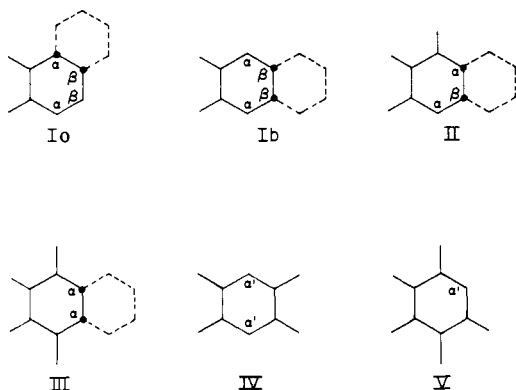


**Figure 2.** Possible ways to attach a reacting ring (dotted) to substrate rings. (Alternative selections for Ia and II may or may not yield new compounds depending on the symmetry of the unshown part of the substrate.)  $\alpha$  sites are one bond removed from a single ring fusion position,  $\beta$  sites are two bonds removed, and  $\alpha'$  sites are one bond removed from two ring fusion positions.

angular ring forming the bay region is known to undergo a series of chemical steps (Figure 1), and quantum chemical calculations<sup>5</sup> suggest that the high reactivity of bay-region PAH may result from the stability of the triol carbonium ion formed relative to the diol epoxide precursor.

The present paper is devoted to an examination of the origin of the unusual stability of bay-region carbonium ion formation. We will show that such carbonium ions are especially stable because the  $-\text{CH}^+$  group can be attached to a carbon atom which is a nearest neighbor to a ring fusion site. PAH not having a bay region are able to place a  $-\text{CH}^+$  group only at carbon atoms which are second nearest neighbors to ring fusion sites. Such carbonium ions are less stabilized by the conjugated ring system.

### Delocalization Energy

It is convenient to mentally divide a candidate PAH molecule into two parts: the ring which we imagine to undergo the chemical changes of Figure 1, which we call the *reacting ring*, and the remainder of the aromatic system, which we call the *substrate*.

We will calculate the  $\pi$  delocalization energy, i.e., the lowering of the total simple Hückel  $\pi$ -electron energy when a substrate becomes a carbonium ion by attachment of a  $\text{CH}_2^+$ . To how many different local alternant substrate topologies can we attach a  $\text{CH}_2^+$ ? The five (I-V) different topologies are shown in Figure 2.  $\alpha$  labels positions which are nearest neighbors to a single

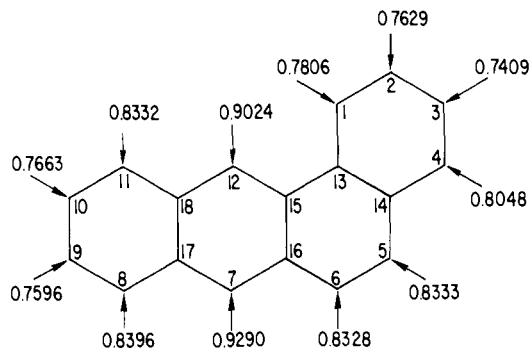


**Figure 3.**  $\Delta E_{\text{deloc}}/\beta$  for formation of carbonium ions by substitution of  $\text{CH}_2^+$  at various sites on benzo[*a*]anthracene.

substrate ring fusion site,  $\beta$  labels those positions which are second nearest neighbors to a ring fusion site, and  $\alpha'$  those positions which are nearest neighbors to two ring fusion sites. Local substrate types IV and V do not provide admissible sites for a reacting ring (Figure 1), since the reacting ring must be joined to the substrate at two adjacent sites, leaving four positions on the reacting ring "open" for diol epoxide formation. However, results associated with attachment at  $\alpha'$  positions will be given since they highlight the importance of neighboring ring fusion sites and could be useful in the interpretation of other chemical phenomena. The three (I, II, and III) admissible substrate types provide a total of four (Ia, Ib, II, and III) topologically distinct choices for placement of the reacting ring (at the dots in Figure 2). A  $-\text{CH}^+$  can be attached at either of the bonds adjacent to the substrate ring as a result of metabolism (step e of Figure 1). It is immediately apparent that, of the various choices, only Ib fails to allow a bay region, and only Ib fails to allow  $-\text{CH}^+$  attachment at an  $\alpha$  position.

Consider, for example, benzo[*a*]anthracene, shown in Figure 3. This molecule can be viewed as the *substrate* for seven other molecules, produced by adding a terminal ring to benzo[*a*]anthracene in any one of seven possible positions (i.e., joining at 1,2; 2,3; 3,4; 5,6; 8,9; 9,10; 10,11). If the ring is added at the 3,4 positions, the resulting molecule is benzo[*b*]chrysene. Upon metabolism of benzo[*b*]chrysene at this terminal ring, we should have the intermediate carbonium ion forming at either position 3 or 4. We have calculated the  $\pi$  delocalization energies associated with the placement of a  $\text{CH}_2^+$  moiety at various positions on benzo[*a*]anthracene. The results, shown with arrows in Figure 3, indicate that a carbonium ion formed at position 4 should be better stabilized by  $\pi$  electron delocalization than one formed at position 3. Therefore, we shall associate the molecule benzo[*b*]chrysene with the delocalization energy 0.8048 $\beta$  on the 4 position of the benzo[*a*]anthracene substrate.

Note that the preference of position 4 over 3 for the carbonium ion, as predicted from Figure 3, is a preference for an  $\alpha$  site over a  $\beta$  site. This order of preference is shown for other sites in this substrate as well. Substitution of  $\text{CH}_2^+$  at  $\beta$  sites (2, 3, 9, or 10) produces less delocalization energy than that at  $\alpha$  sites (1, 4, 5, 6, 8, or 11). Substitution at  $\alpha'$  site (7 or 12) gives greatest delocalization energy, but these sites are not relevant to terminal ring metabolism.

We have calculated delocalization energies for a total of ten substrates. The remaining nine are shown in Figure 4. In general, the relative order seen above for stabilities of  $\text{CH}_2^+$  at  $\beta$ ,  $\alpha$ , and  $\alpha'$  sites is retained throughout all ten substrates. The data are plotted in Figure 5. There is a small region of overlap in delocalization energies for  $\alpha$  and  $\beta$  sites, but the separation is remarkably good. Also plotted in Figure 5 are carcinogenicity data<sup>6</sup> for 23 PAH which would produce carbonium ions having the plotted delocalization energy. As previously mentioned, one can imagine the carbonium ion to form at either of the two sites where

(4) Wood, A. W.; Chang, R. L.; Levin, W.; Ryan, D. E.; Thomas, P. E.; Croisy-Delcey, M.; Ittah, Y.; Yagi, H.; Jerina, D. M.; Conney, A. H. *Cancer Res.* **1980**, *40*, 2876-2883, and references therein. For a critical review of bay region and other theories of carcinogenicity, see B. Pullman, *Int. J. Quantum Chem.* **1979**, *16*, 669-689.

(5) Jerina, D. M.; Lehr, R. E.; Yagi, H.; Hernandez, O.; Dansette, P. M.; Weslocki, P. G.; Wood, A. W.; Chang, R. L.; Levin, W.; Conney, A. H. In "In Vitro Metabolic Activation and Mutagenesis Testing"; de Serres, F.; Fouts, J. R.; Bend, J. R.; Philpot, R. M. eds.; Elsevier: Amsterdam, 1976; pp 159-177.

(6) Jerina, D. M.; Lehr, R. E. In "Microsomes and Drug Oxidation"; Ullrich, V.; Roots, I.; Hildebrandt, A. G.; Estabrook, R. W.; Conney, A. H., Eds; Pergamon Press: Oxford, England, 1977; pp 709-720.

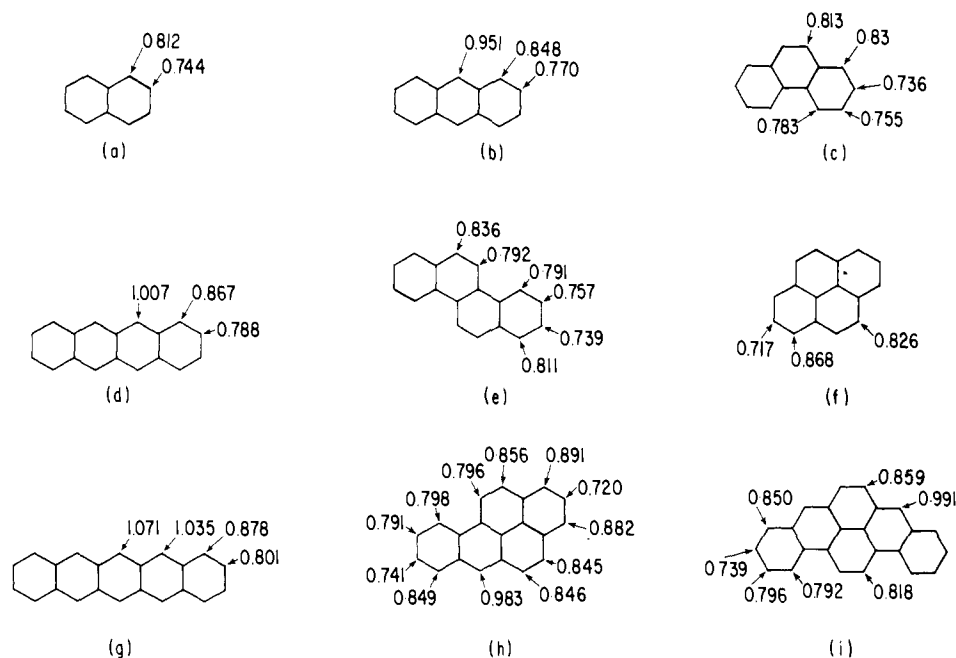


**Figure 4.**  $\Delta E_{\text{deloc}}/\beta$  for nine substrate molecules. Figure 3 provides data for an additional substrate. [Note added in proof: in (c), 0.83 should be 0.803.]

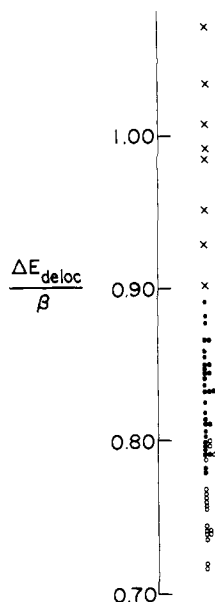


**Figure 5.**  $\pi$  delocalization energy (in units of  $\beta$ ) for  $\text{CH}_2^+$  substitution at various sites on ten substrates.  $\times$  refers to sites  $\alpha'$ , adjacent to two fusion sites;  $\bullet$  refers to positions  $\alpha$ , adjacent to one fusion site;  $\circ$  refers to positions  $\beta$ , adjacent to no fusion sites. The carcinogenicity of associated PAH is indicated as (-) not active, (+) slightly active, (++) fairly active, (+++) very active, or (++++) extremely active. The carcinogenicity symbols correspond, from highest to lowest positions on the figure, to the following parent molecules and substrate delocalization energies (in units of  $\beta$ ): dibenzo[*a,i*]pyrene, (++++) 0.891; dibenzo[*a,h*]pyrene, (++++) 0.882; benzo[*a*]pyrene, (++++) 0.868; benzo[*a*]tetracene, (-) 0.867; tribenzo[*a,e,i*]pyrene, (++) 0.859; dibenzo[*a,l*]pyrene, (++++) 0.856; benzo[*a*]anthracene, (+) 0.848; dibenzo[*a,e*]pyrene, (++++) 0.846; dibenzo[*a,h*]anthracene, (++) 0.8396; benzo[*g*]chrysene, (++) 0.836; dibenzo[*a,j*]anthracene, (+) 0.833; dibenzo[*a,c*]anthracene, (+) 0.833; benzo[*e*]pyrene, (+) 0.8264; triphenylene, (-) 0.813; phenanthrene, (-) 0.812; picene, (-) 0.811; benzo[*b*]chrysene, (-) 0.8048; chrysene, (+) 0.803; naphtho[2,3-*b*]pyrene, (++) 0.791; pentacene, (-) 0.788; benzo[*c*]phenanthrene, (+) 0.783; tetracene, (-) 0.770; anthracene, (-) 0.744.

the reacting ring is attached to the substrate. In each instance, we have chosen the larger of the two possible delocalization energies. The most carcinogenic PAH are those whose bay-region carbonium ions would be stabilized by approximately  $0.83\beta$  or

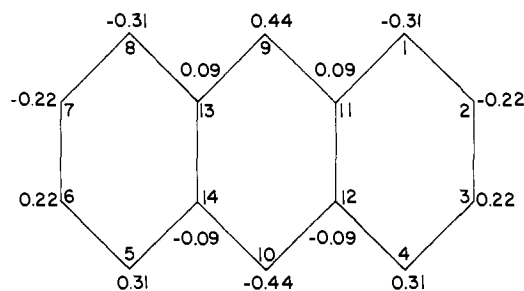


**Figure 6.** The HOMO of anthracene. The fact that the absolute coefficients are largest at position 9 and smallest at position 2 leads to  $\Delta E_{\text{deloc}}$  being largest at 9 and smallest at 2.

greater. (Many more than 23 PAH are related to these ten substrates, but carcinogenicity data are not available for all possibilities.)

#### Perturbation Theory Analysis

In the present section, we will examine the perturbation expression for the delocalization energy and attempt to understand the difference between the  $\alpha$ ,  $\beta$ , and  $\alpha'$  sites. According to standard perturbation treatment,<sup>7</sup> the delocalization energy produced by bringing a  $\text{CH}_2^+$  up to atom  $k$  of a conjugated substrate is approximately:

$$\Delta E_{\text{deloc}} = 2 \sum_i \frac{c_{ik}^2 \beta^2}{\epsilon_i - \alpha} \quad (1)$$

where  $c_{ik}$  is the coefficient for a  $p_\pi$  atomic orbital in the  $i$ th MO at atom  $k$  of the substrate and  $\epsilon_i$  is the energy of that MO. ( $\alpha$  and  $\beta$  in eq 1 are the Hückel coulomb and resonance integrals, respectively, and should not be confused with the  $\alpha$  and  $\beta$  positions we have been referring to.) We have compared the  $\Delta E_{\text{deloc}}$  of eq 1 with that calculated directly and found that the perturbation expression overestimates  $\Delta E_{\text{deloc}}$  by about 20%. Nevertheless, eq 1 does tend to maintain the proper ordering of  $\Delta E_{\text{deloc}}$  for the  $\alpha$ ,  $\beta$ , and  $\alpha'$  sites and is useful in interpreting the origin of carbonium ion stabilization. In particular, eq 1 indicates that a contribution to  $\Delta E_{\text{deloc}}$  is largest when  $|c_{ik}|$  is large and  $\epsilon_i - \alpha$  is small. In other words, the delocalization energy is greatest at sites where the

(7) Dewar, M. J. S. "The Molecular Orbital Theory of Organic Chemistry"; McGraw-Hill: New York, 1969; pp 203-205.

higher energy occupied MOs have their largest coefficients. In some cases, one needs to examine only the highest occupied MO (HOMO) in order to predict qualitatively the variation of  $\Delta E_{\text{deloc}}$  with attachment of  $\text{CH}_2^+$  to different ring positions. Figure 6 gives the HOMO for anthracene. It is clearly largest at position 9 (an  $\alpha'$  position), second largest at position 1 (an  $\alpha$  position), smaller yet at position 2 (a  $\beta$  position), and smallest at the fusion sites themselves (e.g., position 11). Why does this HOMO have these properties? The answer is not very complicated. The more bonding a Hückel MO is, the lower its energy lies (see, for instance, ref 8). Occupied MOs having large coefficients at ring fusion sites 11–14 will tend to get maximum bonding from those coefficients (since such atoms participate in three C–C bonds) and so will tend to be low in energy. Large coefficients at sites like 1 and 2 are less effective at producing bonding because of the smaller number of carbon neighbors. There is, therefore, a tendency for larger coefficients at fusion sites to be concentrated in lower-energy MOs. This means that *highest-energy occupied MOs will tend to have small coefficients at fusion sites*. Now a highest-energy MO will have an energy in the neighborhood of  $\alpha + 0.5\beta$ . The corresponding wave function has a distance between nodes of less than three bonds. This means that, if we know that a HOMO coefficient is very small on one atom, we know it must be quite large on one of the adjacent atoms and of intermediate size at the atom beyond that. Thus, we expect a HOMO to have small coefficients on fusion site atoms, large coefficients at sites  $\alpha$  and  $\alpha'$ , adjacent to fusion sites, and intermediate coefficients at sites  $\beta$  which are second neighbors to fusion sites. The anthracene substrate illustrates this nicely. The origin of the enhanced reactivity of the 3,4-diol and 3,4-diol 1,2-epoxide<sup>9,10</sup> of benzo[*a*]anthracene with respect to other isomeric diols and diol epoxides is then simply understood in terms of the larger HOMO coefficients at positions 1, 4, 5, and 8 on the anthracene substrate, these coefficients being larger because they are nearest neighbors to fusion sites. (It should be pointed out, however, that even though one expects bay-region diol epoxides to be generally the most reactive, this does not preclude the possibility of significant amounts of binding between non-bay-region diol epoxides and DNA.<sup>11</sup>)

A complication arises when the substrate has its fusion sites placed in a manner which makes it impossible for them all to have small coefficients in the same MO. The benzo[*a*]anthracene substrate (Figure 3) is an example. The HOMO for this molecule is given in Figure 7a. The anthracene fragment of this substrate obeys our rules fairly well but there are problems at positions 1–4. Position 1, which is the nearest neighbor to a fusion site (an  $\alpha$  site), has a very small coefficient. This comes about because the carbon atom at position 13 is an  $\alpha'$  site, adjacent to fusion sites 14 and 15 (favoring a large coefficient at site 13) and yet is itself a fusion site (favoring a small coefficient at site 13). The coefficient at position 1 is, therefore, dependent on the decision taken at position 13. The decision not to make the coefficient at site 13 very small leads to a very small coefficient at position 1 in the HOMO. We find, however, that whenever an "identity crisis"

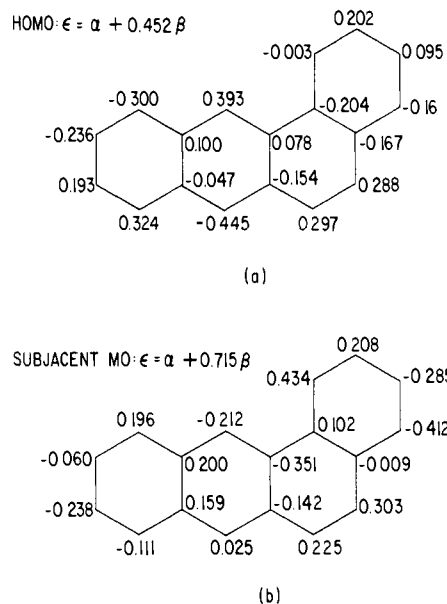


Figure 7. MOs for benzo[*a*]anthracene: (a) the HOMO, (b) the second-highest occupied MO. See Figure 3 for position numbers.

of this sort arises, there is another MO not far below the HOMO which resolves the issue in the reverse way. Figure 7b illustrates the second-highest occupied MO ("subjacent MO") of benzo[*a*]anthracene. Note that the coefficient at position 13 is smaller and that at position 1 is much larger in this MO. This subjacent orbital, therefore, stabilizes  $\text{CH}_2^+$  attachment at position 1. As a result, the values of  $\Delta E_{\text{deloc}}$  (Figure 3) at the  $\alpha$  positions 1 and 4 are larger than at the  $\beta$  positions 2 and 3 despite the fact that the HOMO contributes almost nothing to  $\Delta E_{\text{deloc}}$  at position 1.

The delocalization energies listed in Figures 3 and 4 are exact simple Hückel values. With some exceptions, they fall in the same numerical order as those calculated by approximate methods by others.<sup>6</sup> The major differences involve the substrates pentacene and tetracene, which we find to have relatively less  $\beta$  site delocalization energy than the earlier work suggests. While not relevant to the carcinogenicity problem, we note that the relative stabilities of radicals or carbanions formed by attaching  $\text{CH}_2$  or  $\text{CH}_2^-$  to an alternant PAH substrate should be identical, according to simple Hückel theory, with those found for carbonium ions.

## Conclusions

The bay-region concept has provided an extremely important rule for simple identification of the most highly reactive diol epoxide of a particular PAH. Previous calculations performed on a wide range of PAH have shown that carbonium ions are most easily formed from bay-region diol epoxides. The present paper has been devoted to determining why this is so. We have pointed out that a bay-region PAH is the only kind that can produce a triol carbonium ion which is at an  $\alpha$  site, neighboring a fusion site of the substrate. Delocalization energy calculations indicate that carbonium ions formed at  $\alpha$  sites are more stable than those formed at  $\beta$  sites. This has been shown to result from the fact that the higher-energy occupied MOs tend to have small coefficients at fusion sites and, therefore, large coefficients at  $\alpha$  sites. This, in turn, is forced by the wavelength, or the separation distance, characteristic of Hückel MOs in this energy range.

(8) Lowe, J. P. "Quantum Chemistry"; Academic Press: New York, 1978, pp 219–220.

(9) Levin, W.; Thakker, D. R.; Wood, A. W.; Chang, R. L.; Lehr, R. E.; Jerina, D. M.; Conney, A. H. *Cancer Res.* **1978**, *38*, 1705–1710.

(10) Slaga, T. J.; Huberman, E.; Selkirk, J. K.; Harvey, R. G.; Bracken, W. M. *Cancer Res.* **1978**, *38*, 1699–1704.

(11) Hemminki, K.; Cooper, C. S.; Ribeiro, D.; Grover, P. L.; Sims, P. *Carcinogenesis* **1980**, *1*, 277–285.